Stimulus repetition modulates gamma-band synchronization in primate visual cortex

Nicolas M. Brunet[a,b,1], Conrado A. Bosman[a,c,1], Martin Vinck[d,1], Mark Roberts[a,e], Robert Oostenveld[a], Robert Desimone[f], Peter De Weerd[a,e], and Pascal Fries[a,d,2]

[a]Donders Institute for Brain, Cognition, and Behaviour, Radboud University Nijmegen, 6525 EN Nijmegen, The Netherlands; [b]Department of Neurological Surgery, University of Pittsburgh, Pittsburgh, PA 15213; [c]Cognitive and Systems Neuroscience Group, Swammerdam Institute for Life Sciences, Center for Neuroscience, University of Amsterdam, 1098 XH Amsterdam, The Netherlands; [d]Ernst Strüngmann Institute (ESI) for Neuroscience in Cooperation with Max Planck Society, 60528 Frankfurt, Germany; [e]Department of Cognitive Neuroscience, Faculty of Psychology and Neuroscience, Maastricht University, 6200 MD Maastricht, The Netherlands; and [f]McGovern Institute for Brain Research, Massachusetts Institute of Technology, Cambridge, MA 02139

Edited by Ranulfo Romo, Universidad Nacional Autonóma de México, Mexico City, Mexico, and approved January 20, 2014 (received for review May 23, 2013)

When a sensory stimulus repeats, neuronal firing rate and functional MRI blood oxygen level-dependent responses typically decline, yet perception and behavioral performance either stay constant or improve. An additional aspect of neuronal activity is neuronal synchronization, which can enhance the impact of neurons onto their postsynaptic targets independent of neuronal firing rates. We show that stimulus repetition leads to profound changes of neuronal gamma-band (∼40–90 Hz) synchronization. Electrocorticographic recordings in two awake macaque monkeys demonstrated that repeated presentations of a visual grating stimulus resulted in a steady increase of visually induced gamma-band activity in area V1, gamma-band synchronization between areas V1 and V4, and gamma-band activity in area V4. Microelectrode recordings in area V4 of two additional monkeys under the same stimulation conditions allowed a direct comparison of firing rates and gamma-band synchronization strengths for multiunit activity (MUA), as well as for isolated single units, sorted into putative pyramidal cells and putative interneurons. MUA and putative interneurons showed repetition-related decreases in firing rate, yet increases in gamma-band synchronization. Putative pyramidal cells showed no repetition-related firing rate change, but a decrease in gamma-band synchronization for weakly stimulus-driven units and constant gamma-band synchronization for strongly driven units. We propose that the repetition-related changes in gamma-band synchronization maintain the interareal stimulus signaling and sharpen the stimulus representation by gamma-synchronized pyramidal cell spikes.

adaptation | learning | oscillation | plasticity | priming

Stimulus repetition typically leads to reduced neuronal firing rates and reduced functional MRI blood oxygen level-dependent signals, whereas behavior that is based on stimulus processing is not affected or is enhanced (1). Different models have been proposed to reconcile these behavioral and neurophysiological findings (1). In a "fatigue model," neuronal responses are reduced in proportion to their amplitude, leaving relative response patterns unchanged; in a "sharpening model," neurons that code features irrelevant to identification of a stimulus exhibit repetition suppression, leading to a sparser and sharpened representation of the repeated stimulus; and in a "facilitation model," stimulus repetition leads to faster stimulus processing, and thereby smaller overall neuronal activity. Gotts and coworkers (2–4) suggested a "synchronization model" in which stimulus repetition leads to reduced firing rates accompanied by increased synchronization. The increased synchronization might explain how less-activated neuronal groups can maintain their impact onto postsynaptic neurons and, ultimately, behavior, while reducing metabolic costs at the same time. The synchronization model has received support from a number of studies in human subjects, using source-localized magnetoencephalography. Ghuman et al. (5) report enhanced frontotemporal 14-Hz synchronization for repeated vs. novel stimuli. Gilbert et al. (3) found that stimulus repetition leads to enhanced 5- to 15-Hz power in the right fusiform gyrus and enhanced 15- to 35-Hz power in striate and extrastriate cortex. Corresponding data were also reported for multisite microelectrodes recordings in striate and parietal cortex of awake cats, where von Stein et al. (6) found that interareal alpha-band synchronization was stronger for repeated compared with novel stimuli. The common finding across these studies is enhanced alpha/beta activity or coupling for repeated stimuli. The alpha coupling reported by von Stein et al. (6) occurs in a behavioral context and has a phase relationship and layer specificity that suggests a top-down–directed interaction. Thus, enhanced alpha/beta activity or coupling for repeated stimuli might reflect enhanced top-down signaling, perhaps related to enhanced predictability of repeated stimuli. However, increased synchronization with stimulus repetition according to the model of Gotts and coworkers (2–4) should also serve the maintenance of feedforward signaling of repeated stimuli in the face of reduced firing rates. Feedforward signaling has been strongly linked to local and interareal gamma-band synchronization (7–9). Local gamma-band synchronization likely enhances the postsynaptic impact of the precisely synchronized output spikes (10). Interareal gamma-band synchronization likely aligns excitability cycles such that inputs arrive when postsynaptic target neurons are receptive (11, 12). However, whether multiple presentations of a stimulus result

Significance

When a visual stimulus repeats multiple times, visual cortical neurons show decreasing firing rate responses, yet neither perception nor stimulus-related behavior is compromised. We show that stimulus repetition leads to increased neuronal gamma-band (∼40–90 Hz) synchronization within and between early and higher visual areas. The enhanced gamma-band synchronization likely maintains effective stimulus signaling in the face of dwindling firing rates. We also show that synchronization to the gamma rhythm increases for spikes in general and for those of putative interneurons, whereas it decreases for spikes of putative excitatory neurons if they are not strongly stimulus-driven. Thus, inhibitory interneurons might create increasingly precise gamma-band synchronization, and thereby prune the stimulus representation by pyramidal cells to be sparser and more efficient.

Author contributions: N.M.B., C.A.B., M.R., R.O., R.D., P.D.W., and P.F. designed research; N.M.B., C.A.B., and P.F. performed research; N.M.B., M.V., and P.F. analyzed data; and N.M.B. and P.F. wrote the paper.

The authors declare no conflict of interest.

This article is a PNAS Direct Submission.

Freely available online through the PNAS open access option.

[1]N.M.B., C.A.B., and M.V. contributed equally to this work.

[2]To whom correspondence should be addressed. E-mail: pascal.fries@esi-frankfurt.de.

This article contains supporting information online at www.pnas.org/lookup/suppl/doi:10.1073/pnas.1309714111/-/DCSupplemental.

in enhanced gamma-band synchronization remains unknown (details are provided in *SI Discussion*). We investigated gamma-band synchronization within and between macaque monkey areas V1 and V4 and report that stimulus repetition leads to profound changes in gamma-band synchronization within and between these areas.

Results

We investigated repetition-related changes in gamma-band synchronization in two datasets, each containing data from two awake macaque monkeys (details of stimulus, task, and recording are provided in *Methods*). The first dataset was obtained from two monkeys (monkeys E1 and E2) implanted with an electrocorticographic (ECoG) grid covering many superficial areas, including areas V1 and V4. The second dataset was obtained from two monkeys (monkeys M1 and M2) and was recorded with standard tungsten microelectrodes in area V4. For both datasets, monkeys were fixating while one or two eccentric patches of drifting grating were presented and the monkeys monitored either the fixation point or one of the grating patches.

Stimulus Repetition Leads to Increasing Area V1 Gamma-Band Activity. We sorted trials according to trial number into eight equally sized and nonoverlapping trial bins. For each trial bin, Fig. 1*A* shows a representative raw local field potential (LFP) trace. Traces are from one recording site in area V1 from one recording session in monkey E1. Fig. 1*B* shows the trial bin averages of the absolute and baseline-normalized power spectra and demonstrates that repeated presentations resulted in increasing gamma-band responses. Fig. 1*C* shows the gamma power as a function of trial bin number. Visually induced gamma-band (52–74 Hz) power was highly correlated to the logarithm of the trial bin number (r^2 = 0.98, P = 4.0e-06). Fig. S1 shows the same analysis as in Fig. 1*B* (*Inset*), but averaged over all sites with significant visually driven gamma-band activity and averaged over three sessions. During these recording sessions, the monkey reported color changes of the fixation point, and the peripheral grating stimulus, which induced gamma-band activity, was behaviorally irrelevant. This suggests that the repetition-related gamma increase did not depend on attention being directed to the gamma-inducing stimulus. Gamma-band activity in these sessions was particularly strong because a full-field grating was used (13).

For the following analyses, we will use data from recording sessions during which the monkeys performed a selective visual attention task with grating patches of 3° of visual angle. If not otherwise stated, we use data from the task period when the stimuli were on the screen and attention had been deployed to one of them, and we pool across the two selective attention conditions. Fig. 1*D* depicts the spatial distribution of all ECoG electrodes on the brain of monkey E1, and Fig. 1*E* shows the visually induced gamma-band power change (stimulation vs. baseline, 52–74 Hz) for all ECoG sites. Fig. 1*F* shows the power spectra averaged over the significantly visually driven area V1 sites of monkey E1 for eight nonoverlapping trial bins (62 of a total of 63 sites; details are provided in *Methods*), averaged further across 25 sessions (6,266 trials). Fig. 1*I* shows the average gamma-band power and the corresponding SE across sessions. When the trial bin number was expressed on a logarithmic scale, there was a near-perfect log-linear relation to the gamma increase (r^2 = 0.99, P = 1e-07). Next, we investigated the spatial

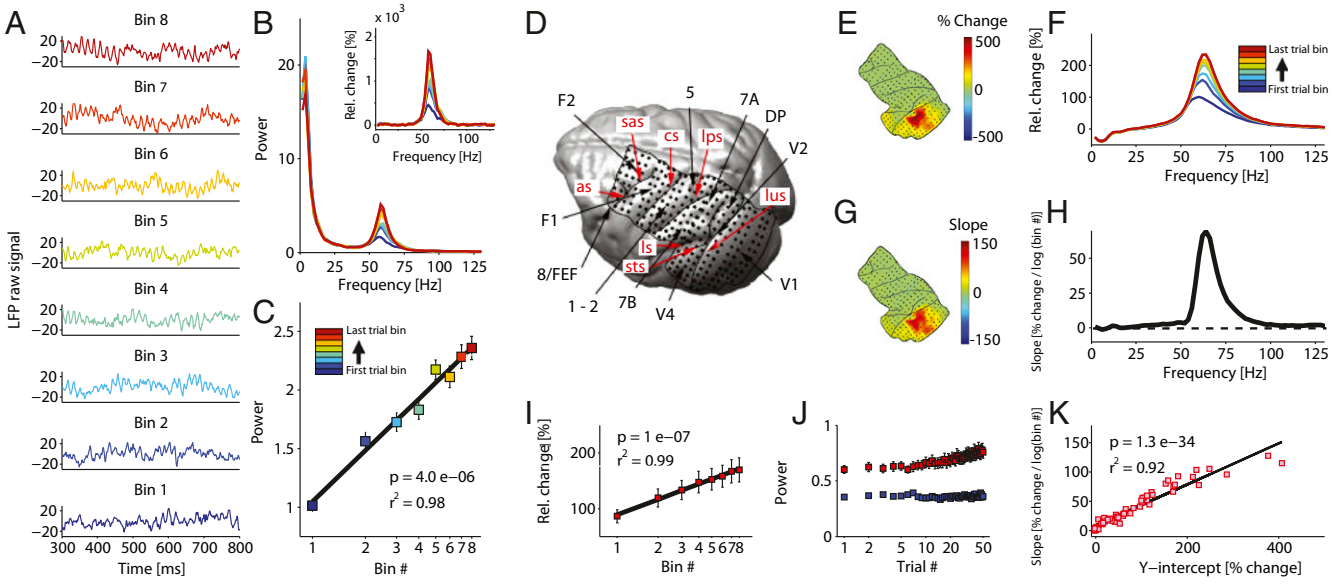

Fig. 1. Stimulus repetition enhances gamma-band activity in visual cortex. (*A*) Raw LFP traces from one representative recording site from area V1 and eight representative trials from one recording session in monkey E1. During this session, monkey E1 performed a color change detection at fixation and the gamma-inducing grating stimulus was behaviorally irrelevant. (*B*) Corresponding absolute and baseline-normalized power spectra. Rel., relative. (*C*) Gamma power as a function of trial bin number on a logarithmic scale. Trials were sorted according to trial number into eight equally sized and nonoverlapping bins, and power was averaged per bin. (*D*) Brain of monkey E1 with ECoG electrodes and major sulci (as, arcuate sulcus; cs, central sulcus; ips, intraparietal sulcus; ls, lateral sulcus; lus, lunate sulcus; sas, spur of the arcuate sulcus; sts, superior temporal sulcus). Black labels point to the covered brain areas. (*E*–*K*) Data from sessions during which monkey E1 performed a selective attention paradigm. (*E*) Relative change in gamma power during stimulation compared with baseline, averaged over all trials. (*F*) Same as in *B* (*Inset*), but averaged over all visually driven area V1 sites and all sessions in monkey E1. Slopes of regression analyses are shown as in *I*, but separately for each site (*G*) and frequency (*H*). (*I*) Same as in *C*, but averaged over area V1 sites and sessions. (*J*) Trial-wise average of gamma-band power for the first 50 trials. Red squares show power during stimulation, and blue squares show power during baseline. (*K*) Each dot corresponds to a visually driven area V1 site in monkey E1. For each site, the regression analysis was performed separately and the scatter plot shows the respective slopes as a function of the intercepts. The intercept estimates the visually induced gamma-band power before the repetition-related increase occurred. This repetition-independent estimate of the stimulus-induced gamma-power change was predictive of the later repetition-related increase. Dots in *D*, *E*, and *G* show electrode positions, yet power estimates are based on sites (i.e., local derivatives). Absolute power values are shown in arbitrary units (a.u.) in *B*, *C*, and *J*.

and spectral specificity of the gamma increase. Fig. 1*G* color-codes the slope of regression lines that were obtained as shown in Fig. 1*I*, but separately for all ECoG sites. The topography of slopes (Fig. 1*G*) was very similar to the topography of visually induced gamma (Fig. 1*E*). This suggests that the increase was specifically related to visually induced activity rather than to drifts in the overall state of the brain or in the recording system. However, Fig. 1*E* shows the visually induced gamma-band activity averaged across all trials (i.e., including later trials in which the visually induced gamma-band activity was already affected by the repetition-related gamma increase). To avoid any circularity and to demonstrate the fine-grained dependence of the repetition-related gamma increase over trials on the visually induced gamma increase within trials, we performed the following analysis. For each of the sites showing clear visually induced gamma, we performed a separate regression analysis and extrapolated the regression line to the *y*-axis intercept for bin number zero, so as to use this intercept as an estimate of the visually induced gamma before any repetition-related increase occurred. We then investigated whether this intercept value predicted the repetition-related regression slope, by calculating a regression between the two parameters. Fig. 1*K* demonstrates a strong correlation (r^2 = 0.92, P = 1.3e-34), confirming that the repetition-related increase was systematically related to the strength of visually induced gamma-band activity. To investigate the spectral specificity of the increase, Fig. 1*H* shows the slopes for the visually driven sites, now as a function of frequency. The slope spectrum demonstrates that the repetition-related increase was specific for the gamma-frequency band, with a spectral shape very similar to the stimulus-induced gamma-power enhancements.

To test whether there was any stimulus-induced gamma-band power in the first few trials of a session, we averaged gamma-band power across sessions separately for each of the first 50 trials (Fig. 1*J*; red squares indicate absolute power during visual stimulation, and blue squares indicate absolute power during prestimulus baseline). This revealed that gamma-band activity was induced already by the very first stimulus presentation of a given session. This analysis also demonstrated that the increase was present for the absolute gamma-band power during visual stimulation (P = 2.8e-20 for monkey E1 and P = 3.5e-11 for monkey E2) and not for the absolute gamma-band power during prestimulus baseline (P = 0.98 for monkey E1 and P = 0.11 for monkey E2). This illustrates that the repetition effect on visually induced gamma power was not due to decreases in prestimulus, but rather to increases in poststimulus gamma-band power. Fig. S2 shows the same analysis for monkey E2, demonstrating a remarkable consistency across the two animals. In monkey E2, 39 area V1 sites were significantly stimulus-driven (of a total of 40 sites), nine recording sessions had been obtained (3,511 trials), and the gamma-frequency band extended from 68 to 82 Hz.

The fact that gamma increased with stimulus repetition both when the stimulus was a large unattended grating and when it was a smaller attended grating suggested that the effect did not depend on attention. We performed an additional analysis in this regard by analyzing the period when visual stimuli were already on the screen but no attentional cue had been given yet. Consistent with the other results, this showed the repetition-related gamma increase (Fig. S3). We also considered that the repetition-related increase was modulated by switches in stimulus features or in the allocation of attention. The respective analyses (Fig. S4) revealed only that the repetition-related increase was slightly larger for repetitions that involved a change in stimulus color, an effect that might be related to predictive coding (14).

Stimulus Repetition Leads to Increasing Area V1–V4 Gamma Coherence and Area V4 Gamma Activity. Gamma power in one area might contribute to communication with connected areas through interareal coherence (7, 8, 11, 12, 15, 16). Therefore, we tested whether the increase was also present for the coherence between area V1 and area V4. All analyses were done after bipolar derivation, thereby excluding a common reference, which can otherwise lead to artifactual coherence estimates. Fig. 2*A* (*Inset*) shows the anatomical definition of area V1 (pink) and area V4 (blue) in monkey E1 (*Methods*). Fig. 2*A* shows the interareal coherence for the eight trial bins averaged over all sessions in this monkey, revealing that interareal coherence also increased monotonically with trial number (62 significantly stimulus-driven area V1 sites of a total of 63 sites and 16 significantly stimulus-driven area V4 sites of a total of 17 sites, 992 interareal site pairs, and 6,266 trials). We performed the same regression analysis as for power, and we plot the resulting slope spectrum in Fig. 2*B*. The dominant result was a coherence increase in the gamma-frequency band. In addition, there was a smaller decrease in a theta-frequency band.

Enhanced gamma coherence between areas V1 and V4 is expected to result in enhanced gamma power in area V4 (12). Fig. 2*C* shows LFP power spectra from area V4 of monkey E1 (16 significantly stimulus-driven sites of a total of 17 sites and 6,266 trials), and Fig. 2*D* shows the corresponding slope spectra, confirming a repetition-related increase in area V4 power in the gamma-frequency band. Fig. S5 shows the repetition-related changes in area V1–V4 coherence and area V4 power for monkey E2, demonstrating that the gamma increase was consistent across the two animals (39 significantly stimulus-driven area V1 sites of a total of 40 sites, 16 significantly stimulus-driven area V4 sites of a total of 17 sites, 624 site pairs, and 3,511 trials).

We considered that the increases in local and long-range gamma-band synchronization could be related to changes in behavior. Therefore, we analyzed behavioral parameters in the same way as power and coherence, by binning trials and performing a regression analysis. This did not reveal any significant effect for response accuracy, for reaction times, or for the rate of microsaccades.

Stimulus Repetition Leads to Increases in the Gamma-Peak Frequency. Recent studies have shown that not only the strength but also the frequency of gamma-band activity can change systematically (e.g., with contrast) (8, 17). Correspondingly, we investigated the gamma

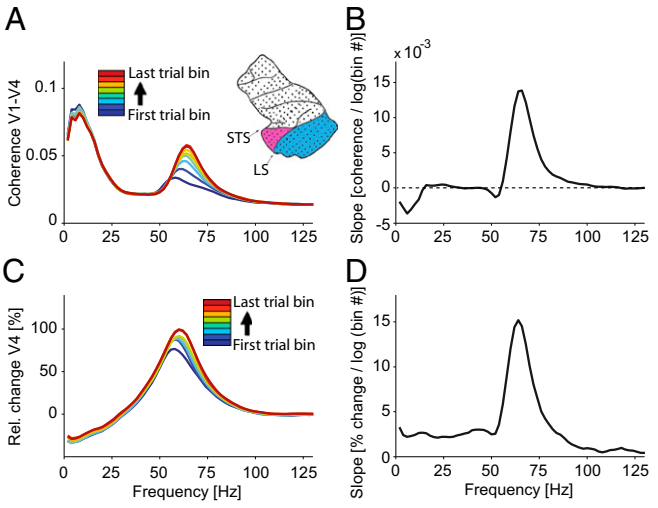

Fig. 2. Stimulus repetition enhances gamma-band coherence between areas V1 and V4 and the gamma-band power in area V4. (*A*) Coherence spectra for monkey E1, averaged over 25 recording sessions and all possible pairs of interareal sites. (*Inset*) Monkey E1 areas V1 (blue) and V4 (pink). LS, lunate sulcus; STS, superior temporal sulcus. (*B*) Slope of the regression of coherence vs. log(trial bin number) as a function of frequency. (*C* and *D*) Same as in *A* and *B*, but for V4 power.

frequency. Fig. S6 shows that for area V1 power, area V1–V4 coherence, and area V4 power, stimulus repetition makes the center of mass of the gamma band move to higher frequencies. This holds for both monkeys.

Stimulus Repetition Leads to Increasing MUA-LFP Synchronization in Area V4. Next, we investigated whether the increases in area V1 gamma power, area V1–V4 gamma coherence, and area V4 gamma power were also reflected in the gamma-band spike-LFP synchronization in area V4. To this end, we analyzed another dataset (monkeys M1 and M2) in which single-unit activity (SUA), multiunit activity (MUA), and LFPs were recorded from four electrodes simultaneously in awake monkey area V4, with electrodes spaced horizontally by 650 or 900 μm. Fig. 3 shows the effects of stimulus repetition on a sample MUA recording and its MUA-LFP synchronization. Fig. 3*A* shows that the firing rate of this MUA declined substantially over the course of 600 stimulus repetitions. Fig. 3 *B* and *C* illustrates that at the same time, the MUA synchronization to the LFP gamma rhythm increased. This is quantified in Fig. 3*D* by the pairwise phase consistency (PPC) between MUA (recorded on one electrode) and the LFP (combined across the other electrodes). The PPC is a recently introduced synchronization metric (18, 19) that avoids any bias by trial number, spike number, or spike rate (details are provided in *Methods*). To avoid strong nonstationarities, the first 0.3 s after stimulus onset was excluded. Fig. 4*A* shows the MUA-LFP PPC using the same data epoch as Fig. 3*D* and the same trial-binning approach as for power and interareal coherence, averaged across all MUA-LFP pairs of both monkeys. Averaging over both monkeys was possible because their gamma-frequency bands were largely overlapping (40–60 Hz) (20). Stimulus repetition led to a clear increase in gamma-band MUA-LFP synchronization, which was highly significant in the regression analysis (Fig. 4*B*; $r^2 = 0.91$, $P = 2.5\text{e-}04$; $n = 109$). Fig. 4*C* shows the regression slopes as a function of frequency and demonstrates that the increase was selectively present in the gamma-frequency band, whereas a low theta band showed a decrease. Fig. S7 demonstrates that this result was consistent across the two monkeys. Enhanced gamma-band MUA-LFP synchronization does not necessarily entail enhanced MUA rates (21), and previous demonstrations of repetition-related firing rate decreases in inferotemporal cortex (22–24) suggest that similar decreases might occur in area V4. Fig. 4*D* shows the normalized MUA rates (±1 SEM) averaged across all sites and sessions in both monkeys M1 and M2. There was a highly significant decrease of MUA firing rates with increasing trial number ($r^2 = 0.94$, $P = 8.2\text{e-}05$).

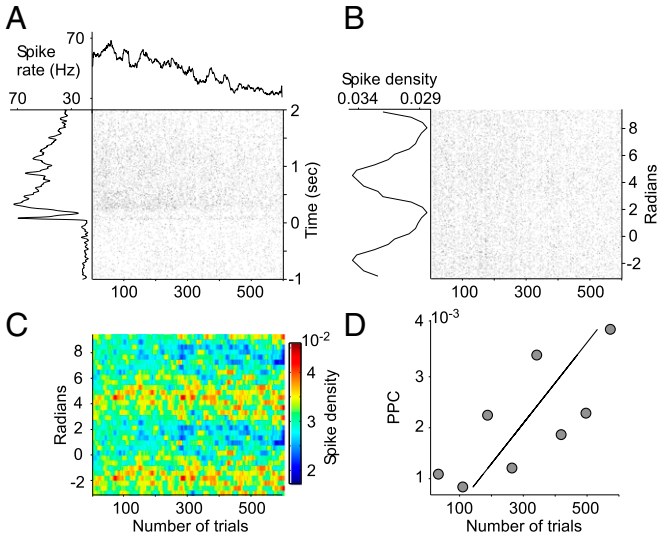

Fig. 3. Evolution of firing rate and spike-LFP phase synchronization for a sample multiunit response. (*A*) Spike rate as a function of time relative to stimulus onset (*Left*) and as a function of trial number (*Upper*, moving average across 15 subsequent trials). (*Right*) Spike rasters of single trials, with each dot corresponding to a spike. Note that we show poststimulus time up to 2 s after stimulus onset, yet target or distracter changes and corresponding trial ending could occur before that. If a trial ended earlier than 2 s after stimulus onset, the remaining time of that trial is discarded. (*B*, *Left*) Spike density (a.u.) as a function of LFP gamma (50 Hz) phase. Spike density was computed using a histogram with 16 bins and then ensuring that the densities plotted sum to 1. (*B*, *Right*) Spike rasters of single trials, with each dot corresponding to a spike. All spikes of a given trial (from 0.3 s poststimulus onset until one of the stimuli changed) are displayed in the corresponding column, irrespective of trial length and resulting number of gamma cycles. As a result, longer trials lead to stronger filling of the column with spikes. *A* and *B* are provided at high resolution in Fig. S9. (*C*) Spike density as a function of LFP gamma (50 Hz) phase, calculated as a moving average across 15 subsequent trials. (*D*) Gamma-band (50 Hz) spike-LFP PPC values for eight nonoverlapping trial bins. The x value of each dot indicates the mean trial number of the respective bin.

Stimulus Repetition Modifies Spike-LFP Synchronization in a Cell Class-Specific Way. In area V4, single units could be sorted, based on their waveforms, into narrow-spiking (NS) cells, which are putative interneurons, and broad-spiking (BS) cells, which are putative pyramidal cells (25, 26). We performed such a differentiation and analyzed firing rates and gamma-band synchronization separately for the two cell groups. Fig. 4*E* shows the average waveforms and the waveform duration histogram for the available single units, sorted into NS cells (red) and BS cells (blue). Fig. 4*F* shows the SUA-LFP PPC in the gamma-frequency band (difference relative to the first trial bin) separately for NS and BS cells: Gamma synchronization increased for the NS cells ($r^2 = 0.8$, $P = 0.003$; $n = 16$) and showed a strong tendency to decrease for the BS cells ($r^2 = 0.5$, $P = 0.05$; $n = 26$). Fig. 4*G* shows the corresponding spike rates; interestingly, the firing rates of NS cells decreased ($r^2 = 0.55$, $P = 0.035$), whereas there was no significant change in BS cell firing rates.

To reconcile the decreasing BS cell gamma synchronization with the increasing MUA gamma synchronization, we reasoned that weakly active and/or weakly stimulus-driven BS cells, which contribute fewer spikes to the MUA, might show strong decreases in synchronization, whereas strongly active and/or strongly driven BS cells, which contribute more spikes to the MUA, might show fewer decreases or even increases in synchronization. To test this hypothesis, we calculated a multiple linear regression between the firing rate and the regression slope. Concretely, we defined the independent firing rate (FR) variables [$FR_{baseline}$] and [$FR_{stimulation}/FR_{baseline}$] and the dependent variable [slope of the regression between synchronization strength and log (repetition bin number)]. Fig. 4*H* shows in blue the *t* values of this multiple linear regression for the BS cells. The dark blue line is for the independent variable [$FR_{stimulation}/FR_{baseline}$] and reveals that, indeed, when a BS cell was more strongly stimulus-driven, it showed a more positive slope of the repetition-related gamma change ($P = 0.0042$). The same analysis for the NS cells (Fig. 4*H*, red lines) did not reveal significant effects. To follow up the result for the BS cells, we performed a median split based on the stimulus-driven firing rate change and averaged the PPC vs. repetition slopes separately for the two groups of cells. This revealed a significant negative slope for the weakly driven BS cells ($P = 0.015$; mean slope ± SEM = −0.0028 ± 0.001) and an absence of a significant repetition-related change for the strongly driven BS cells ($P = 0.9$; mean slope ± SEM = 0.0001 ± 0.0001). We also sorted the BS cells into those with a decreasing slope ($n = 15$; three cells were individually significant) and those with an increasing slope ($n = 11$; one cell was individually significant).

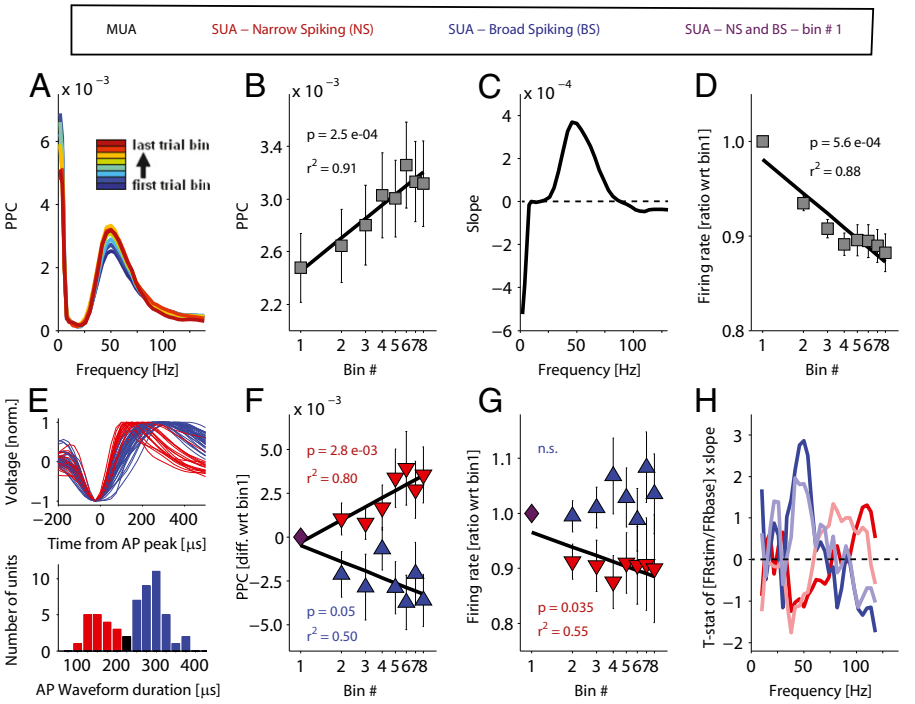

Fig. 4. Effect of stimulus repetition on the gamma-band spike-LFP synchronization. (*A*) PPC of multiunit spikes with regard to the spectral phase of the LFP recorded on neighboring electrodes (details are provided in *Methods*). (*B*) PPC from *A* as a function of trial bin number. (*C*) Slopes of regression analyses as shown in *B*, as a function of frequency. (*D*) Ratio of MUA firing rate with regard to the first trial bin, as a function of trial bin number, and the corresponding regression analysis. (*E*) Spike waveforms (averages per isolated single unit) and the distribution of the corresponding action potential waveform durations. Neurons with waveform durations in the black bin were discarded. norm., normal. (*F*) Change in PPC with regard to the first trial bin (diff. wrt bin 1), separately for NS and BS cells. (*G*) Ratio of the firing rate with regard to the first trial bin (ratio wrt. bin 1), separately for NS and BS cells. (*H*) Regression *t* statistics from two separate multiple linear regression analyses for the BS and NS cells, respectively. The multiple linear regressions fitted the dependent variable [slope of the regression between spike-LFP PPC and log(trial bin number)] as a function of the independent variables (firing rate in the baseline), with results shown as softly colored lines, and [firing rate during stimulation (FRstim)/firing rate in the baseline (FRbase)] NS (BS) waveforms. All panels show grand averages of all microelectrode recordings (i.e., averages across monkeys M1 and M2, across all recordings sessions, and across all sites or units, respectively). All recording sites were in area V4.

The index $[(FR_{stimulation} - FR_{baseline})/(FR_{stimulation} + FR_{baseline})]$ was, on average, 0.23 ± 0.12 for BS cells with negative slope and 0.49 ± 0.11 for BS cells with positive slope (difference not significant).

Discussion

We found that in the course of a recording session, during repeated stimulus presentations, gamma-band activity in area V1 increased by approximately a factor of 2. The strength of gamma-band activity was linearly related to the logarithm of the repetition bin number. This repetition-related gamma increase was spatially specific for the sites with visually induced gamma, and the strength of the repetition-related increase was systematically related to the strength of the visually induced gamma before any repetition-related increase. Furthermore, the repetition-related gamma increase did not appear to be dependent on selective visual attention. A very similar repetition-related increase was also present for the interareal gamma-band coherence between areas V1 and V4 and for the gamma-band activity in area V4. In a separate dataset from area V4, we showed that multiunit synchronization to the gamma rhythm increased by roughly 30%, whereas the multiunit rate decreased by roughly 12%. When separating single units into BS and NS cells, the NS cells showed qualitatively the same synchronization and rate changes as the multiunit. The BS cells showed a strong trend for a repetition-related decrease in gamma synchronization, which was significant for the weakly stimulus-driven cells but absent for the strongly driven ones.

Repetition-related increases in area V1 gamma-band activity and area V1–V4 gamma-band synchronization are expected to lead to an increasing impact of area V1 input onto area V4 (7, 11, 12). Because this increasing impact is rhythmic in the gamma-frequency band, it is expected to result, in area V4, in increasing gamma-band activity and increasing gamma spike-field synchronization but not necessarily in increasing overall firing rates, in line with the results reported here. It is conceivable that the overall firing rate decrease in area V4 is related to the increased gamma-rhythmic impact and the increased local gamma spike-field synchronization. We have shown previously that spikes that are maximally synchronized to the local gamma rhythm are more stimulus-selective than less gamma-synchronized spikes (27). With repeating stimulation, increasing area V1–V4 coherence, and corresponding impact, the less gamma-synchronized spikes in area V4 seem to disappear, leaving the more gamma-synchronized spikes from the more stimulus-driven neurons (Fig. 4*H*). The precise mechanisms of this pruning of non–gamma-synchronized spikes are unclear. They might well be a consequence of the increasing gamma-band synchronization, or they might be independent of the mechanisms behind gamma and its repetition-related increase.

From a methodological point of view, the present results are important for the interpretation of previous studies and for the optimal design of future studies on gamma-band synchronization. Typically, neurophysiological studies use multiple repetitions of a given experimental condition. Where previous studies confounded their experimental conditions with repetitions (e.g., by presenting conditions in blocks of trials without sufficient counterbalancing), this might have resulted in apparent condition effects that actually were repetition effects. Where previous studies properly randomized conditions across repetitions, the repetition-related effect described here might have led to an underestimation of the significance and/or size of the effect of the respective experimental conditions. For future studies on gamma-band synchronization, the present results emphasize the importance of proper condition randomization in the experiment design and of taking repetitions into account in the data analysis. A discussion of related studies (22–24, 28–36) is provided in *SI Discussion* and Fig. S8.

In Fig. 4, we analyzed the changes in gamma synchronization separately for MUA, NS cells, and BS cells. NS cells are putative interneurons, although this cannot be proven in the awake monkey preparation at this moment. Networks of interneurons are the core generators of gamma-band synchronization (26, 37). Consistent with this, the gamma synchronization of the NS cells

increased similar to the gamma power/coherence within/between ECoG signals. Intriguingly, the BS cells showed repetition-related changes in gamma synchronization that depended on their stimulus-driven activation. Weakly driven BS cells showed repetition-related decreases in gamma synchronization, whereas strongly driven BS cells kept their gamma synchronization unchanged across repetitions. Thus, across repetitions, the gamma-synchronized spike output contained fewer and fewer spikes from weakly stimulus-driven BS cells and relatively more spikes from strongly stimulus-driven BS cells, which amounts to a sharpening of the stimulus representation in the gamma-synchronized spike output (27). We have recently described a very similar effect of selective attention on cell type-specific gamma-band synchronization (26). It is particularly the gamma-synchronized spikes that have an impact on postsynaptic target neurons, and in this postsynaptic target group of neurons, the different input neurons always mutually reduce impact through normalization mechanisms (38). Thus, if the gamma-synchronized spike output contains relatively more spikes from strongly stimulus-driven BS cells, this lends those cells a stronger effective impact.

Methods

A detailed description of the methods used in this study is provided in *SI Methods*. If not stated otherwise, data are from recording sessions in which the monkeys performed a selective visual attention task. They kept fixation on a central dot while two patches of drifting grating were presented, of which one fell into the receptive field of the recorded neurons. In monkeys E1 and E2, ECoG grid electrodes were implanted over the left hemisphere to obtain LFPs (7, 39, 40). We use electrodes over areas V1, V2, and V4 and the temporal-occipital area (TEO). When we refer to area V1 (V4), this also includes some electrodes that might be over area V2 (TEO). LFPs from immediately neighboring electrodes were subtracted to obtain local bipolar derivations, which avoid a common reference in interareal coherence analysis. In monkeys M1 and M2, standard techniques were used to record with four microelectrodes simultaneously in visual area V4 (20, 41).

ACKNOWLEDGMENTS. We thank Edward Chang for help with implanting monkey E2, Paul Gaalman for help with structural MRI recordings, and Wolf Singer and Alina Peter for helpful comments to earlier versions of this manuscript. This work was supported by Human Frontier Science Program Organization Grant RGP0070/2003 (to P.F.); Volkswagen Foundation Grant I/79876 (to P.F.); the European Science Foundation's European Young Investigator Award Program (to P.F.); a European Union HEALTH-F2-2008-200728 Grant (to P.F.); the Landes-Offensive zur Entwicklung Wissenschaftlich-ökonomischer Exzellenz program grant "Neuronale Koordination Forschungsschwerpunkt Frankfurt" (to P.F.); the Smart Mix Programme of the Netherlands Ministry of Economic Affairs and the Netherlands Ministry of Education, Culture, and Science (BrainGain) (P.F. and R.O.); and The Netherlands Organization for Scientific Research Grant 452-03-344 (to P.F.).

1. Grill-Spector K, Henson R, Martin A (2006) Repetition and the brain: Neural models of stimulus-specific effects. *Trends Cogn Sci* 10(1):14–23.
2. Gotts SJ (2003) *Mechanisms Underlying Enhanced Processing Efficiency in Neural Systems* (Carnegie Mellon University, Pittsburgh).
3. Gilbert JR, Gotts SJ, Carver FW, Martin A (2010) Object repetition leads to local increases in the temporal coordination of neural responses. *Front Human Neurosci* 4:30.
4. Gotts SJ, Chow CC, Martin A (2012) Repetition Priming and Repetition Suppression: A Case for Enhanced Efficiency Through Neural Synchronization. *Cogn Neurosci* 3(3-4): 227–237.
5. Ghuman AS, Bar M, Dobbins IG, Schnyer DM (2008) The effects of priming on frontal-temporal communication. *Proc Natl Acad Sci USA* 105(24):8405–8409.
6. von Stein A, Chiang C, König P (2000) Top-down processing mediated by interareal synchronization. *Proc Natl Acad Sci USA* 97(26):14748–14753.
7. Bosman CA, et al. (2012) Attentional stimulus selection through selective synchronization between monkey visual areas. *Neuron* 75(5):875–888.
8. Roberts MJ, et al. (2013) Robust gamma coherence between macaque V1 and V2 by dynamic frequency matching. *Neuron* 78(3):523–536.
9. Buffalo EA, Fries P, Landman R, Buschman TJ, Desimone R (2011) Laminar differences in gamma and alpha coherence in the ventral stream. *Proc Natl Acad Sci USA* 108(27): 11262–11267.
10. Azouz R, Gray CM (2003) Adaptive coincidence detection and dynamic gain control in visual cortical neurons in vivo. *Neuron* 37(3):513–523.
11. Fries P (2005) A mechanism for cognitive dynamics: Neuronal communication through neuronal coherence. *Trends Cogn Sci* 9(10):474–480.
12. Womelsdorf T, et al. (2007) Modulation of neuronal interactions through neuronal synchronization. *Science* 316(5831):1609–1612.
13. Gieselmann MA, Thiele A (2008) Comparison of spatial integration and surround suppression characteristics in spiking activity and the local field potential in macaque V1. *Eur J Neurosci* 28(3):447–459.
14. Bastos AM, et al. (2012) Canonical microcircuits for predictive coding. *Neuron* 76(4): 695–711.
15. Schoffelen JM, Oostenveld R, Fries P (2005) Neuronal coherence as a mechanism of effective corticospinal interaction. *Science* 308(5718):111–113.
16. Schoffelen JM, Poort J, Oostenveld R, Fries P (2011) Selective movement preparation is subserved by selective increases in corticomuscular gamma-band coherence. *J Neurosci* 31(18):6750–6758.
17. Ray S, Maunsell JH (2010) Differences in gamma frequencies across visual cortex restrict their possible use in computation. *Neuron* 67(5):885–896.
18. Vinck M, van Wingerden M, Womelsdorf T, Fries P, Pennartz CM (2010) The pairwise phase consistency: A bias-free measure of rhythmic neuronal synchronization. *Neuroimage* 51(1):112–122.
19. Vinck M, Battaglia FP, Womelsdorf T, Pennartz C (2012) Improved measures of phase-coupling between spikes and the Local Field Potential. *J Comput Neurosci* 33(1): 53–75.
20. Fries P, Womelsdorf T, Oostenveld R, Desimone R (2008) The effects of visual stimulation and selective visual attention on rhythmic neuronal synchronization in macaque area V4. *J Neurosci* 28(18):4823–4835.
21. Fries P, Roelfsema PR, Engel AK, König P, Singer W (1997) Synchronization of oscillatory responses in visual cortex correlates with perception in interocular rivalry. *Proc Natl Acad Sci USA* 94(23):12699–12704.
22. Sobotka S, Ringo JL (1994) Stimulus specific adaptation in excited but not in inhibited cells in inferotemporal cortex of macaque. *Brain Res* 646(1):95–99.
23. Li L, Miller EK, Desimone R (1993) The representation of stimulus familiarity in anterior inferior temporal cortex. *J Neurophysiol* 69(6):1918–1929.
24. Miller EK, Li L, Desimone R (1993) Activity of neurons in anterior inferior temporal cortex during a short-term memory task. *J Neurosci* 13(4):1460–1478.
25. Mitchell JF, Sundberg KA, Reynolds JH (2007) Differential attention-dependent response modulation across cell classes in macaque visual area V4. *Neuron* 55(1): 131–141.
26. Vinck M, Womelsdorf T, Buffalo EA, Desimone R, Fries P (2013) Attentional modulation of cell-class-specific gamma-band synchronization in awake monkey area v4. *Neuron* 80(4):1077–1089.
27. Womelsdorf T, et al. (2012) Orientation selectivity and noise correlation in awake monkey area V1 are modulated by the gamma cycle. *Proc Natl Acad Sci USA* 109(11): 4302–4307.
28. van Wingerden M, Vinck M, Lankelma JV, Pennartz CM (2010) Learning-associated gamma-band phase-locking of action-outcome selective neurons in orbitofrontal cortex. *J Neurosci* 30(30):10025–10038.
29. van Wingerden M, et al. (2012) NMDA receptors control cue-outcome selectivity and plasticity of orbitofrontal firing patterns during associative stimulus-reward learning. *Neuron* 76(4):813–825.
30. Stopfer M, Laurent G (1999) Short-term memory in olfactory network dynamics. *Nature* 402(6762):664–668.
31. Ringo JL (1996) Stimulus specific adaptation in inferior temporal and medial temporal cortex of the monkey. *Behav Brain Res* 76(1-2):191–197.
32. Wang Y, Iliescu BF, Ma J, Josić K, Dragoi V (2011) Adaptive changes in neuronal synchronization in macaque V4. *J Neurosci* 31(37):13204–13213.
33. Kaliukhovich DA, Vogels R (2012) Stimulus repetition affects both strength and synchrony of macaque inferior temporal cortical activity. *J Neurophysiol* 107(12): 3509–3527.
34. Huber R, et al. (2013) Human cortical excitability increases with time awake. *Cereb Cortex* 23(2):332–338.
35. Vinck M, et al. (2010) Gamma-phase shifting in awake monkey visual cortex. *J Neurosci* 30(4):1250–1257.
36. Friese U, Supp GG, Hipp JF, Engel AK, Gruber T (2012) Oscillatory MEG gamma band activity dissociates perceptual and conceptual aspects of visual object processing: A combined repetition/conceptual priming study. *Neuroimage* 59(1):861–871.
37. Buzsáki G, Wang XJ (2012) Mechanisms of gamma oscillations. *Annu Rev Neurosci* 35: 203–225.
38. Reynolds JH, Chelazzi L, Desimone R (1999) Competitive mechanisms subserve attention in macaque areas V2 and V4. *J Neurosci* 19(5):1736–1753.
39. Brunet N, et al. (2013) Visual cortical gamma-band activity during free viewing of natural images. *Cereb Cortex*, 10.1093/cercor/bht280.
40. Rubehn B, Bosman C, Oostenveld R, Fries P, Stieglitz T (2009) A MEMS-based flexible multichannel ECoG-electrode array. *J Neural Eng* 6(3):036003.
41. Fries P, Reynolds JH, Rorie AE, Desimone R (2001) Modulation of oscillatory neuronal synchronization by selective visual attention. *Science* 291(5508):1560–1563.